Available online at www.sciencedirect.com

SCIENCE DIRECT

OCEAN ENGINEERING

Ocean Engineering 32 (2005) 195–222

www.elsevier.com/locate/oceaneng

Bottom friction caused by boundary layer streaming beneath random waves for laminar and smooth turbulent flow

Dag Myrhaug*, Lars Erik Holmedal

Department of Marine Technology, Norwegian University of Science and Technology, NO-7491 Trondheim, Norway

Received 16 January 2004; accepted 2 June 2004
Available online 26 October 2004

Abstract

The effect of boundary layer streaming on the sea bed shear stresses, beneath random waves, is investigated for laminar flow as well as smooth turbulent flow. It is demonstrated how bottom friction formulas for regular waves can be used to obtain the bed shear stresses resulting from steady streaming under random waves. As a result, friction factors for steady streaming under random waves are provided, and the effect of streaming versus the effect of linear waves is discussed. For laminar flow the effect of second order Stokes waves is also included. Examples are included to illustrate the applicability of the present practical method, and results are obtained using data typical for field conditions.

Keywords: Random waves; Streaming; Bottom friction; Laminar flow; Smooth turbulent flow; Stochastic approach

1. Introduction

The steady streaming under sinusoidal waves is caused by the non-uniformity of the wave boundary layer resulting from spatial changes of the orbital velocities. This non-uniformity of progressive waves causes a change in the mean shear stress over the wave

* Corresponding author. Tel.: +47 7359 5527; fax: +47 7359 5528.
E-mail address: dagmyr@marin.ntnu.no (D. Myrhaug).

0029-8018/$ - see front matter
doi:10.1016/j.oceaneng.2004.06.011

boundary layer. The steady streaming for a laminar wave boundary layer was determined by Longuet-Higgins (1956). Based on this work the streaming-related time-averaged bed shear stress can be expressed in terms of the wave friction factor and the wave number (see e.g. Nielsen, 1992). Recently Nielsen and Callaghan (2003) included the effect of streaming predicting the shear stress and the total sediment transport rate for sheet flow under waves. Here the effect of streaming was included by adding a constant shear stress corresponding to the streaming-related bed shear stress, and by applying the friction factor for rough turbulent flow. This method predicts the real propagating wave observations of Ribberink et al. (2000) quite well. A summary of results from models and experiments on wave-induced streaming near the seabed is given by Davies and Villaret (1997, 1998, 1999). Above a smooth bed the measured streaming at the edge of the wave boundary layer is in reasonable agreement with the predictions by Longuet-Higgins (1956).

The purpose of this paper is to investigate the effect of streaming on the bed shear stresses beneath random waves for laminar and smooth turbulent flow, and to compare the magnitude of these streaming-related bed shear stresses with those for linear waves. This is of practical interest for, e.g. flow over smooth and featureless beds as is frequently the case for freshly deposited muds, which are commonly taken to be smooth turbulent (Whitehouse et al., 2000, p. 52). The bed shear stresses enter in the calculating of, e.g. erosion and deposition rates of mud. The present analysis also has physical implications for, e.g. estimation of wave energy dissipation for flow above such beds. Specifically, the cumulative distribution function of bed shear stresses related to streaming of individual random waves is determined; characteristic statistical values are calculated, and the root-mean-square (rms) friction factors for random waves are provided. The effect of streaming versus the effect of linear waves is investigated. For laminar flow the effect of second order Stokes waves is also included. Thus two second order effects are considered for laminar flow, as streaming is a second order effect of linear waves. Streaming under second order Stokes waves is not considered here; that would imply including terms of similar or smaller magnitude. Finally, examples of the calculation procedure are given.

Previous studies of bottom friction beneath random waves have been undertaken; a brief review is given by Myrhaug and Holmedal (2003). Myrhaug and Holmedal (2002) used a rough turbulent bed friction formula valid for regular second order Stokes waves to find the cumulative distribution function of individual bed shear stress maxima for nonlinear random waves plus a weak current. The friction factor for random waves, in the lower near-bed excursion amplitude to bed roughness ratio range, was given. In a proceeding paper, Myrhaug and Holmedal (2003) used a similar approach to calculate the laminar bottom friction beneath nonlinear random waves. An extension to nonlinear random waves plus current flow was also suggested.

2. Effect of streaming under random waves

2.1. Theoretical background for regular waves

Following Nielsen (1992) the bottom shear stress related to the wave-induced current (streaming) in the laminar bottom boundary layer of regular waves is given as follows

$$\frac{\tau_{\mathrm{str}}}{\rho} = \frac{1}{2\sqrt{2}} k \sqrt{\frac{\nu}{\omega}} U^2 \tag{1}$$

where U is the near-bed orbital velocity amplitude, ω is the angular wave frequency, ρ is the density of the fluid, ν is the kinematic viscosity of the fluid, k is the wave number determined from the dispersion relationship $\omega^2 = gk \tanh kh$, g is the acceleration of gravity, and h is the water depth. Eq. (1) can be re-arranged as

$$\frac{\tau_{\mathrm{str}}}{\rho} = \frac{1}{4\sqrt{2}} kA^3\omega^2 f_{\mathrm{w}} = \frac{1}{4\sqrt{2}} kAf_{\mathrm{w}} U^2 \tag{2}$$

where $A = U/\omega$ is the near-bed orbital displacement amplitude, and f_{w} is the laminar wave friction factor given as that for Stokes' second problem (Schlichting, 1979)

$$f_{\mathrm{w}} = 2Re^{-0.5} \quad \text{for } Re \lesssim 3 \times 10^5 \tag{3}$$

where

$$Re = \frac{UA}{\nu} \tag{4}$$

is the Reynolds number associated with the wave motion.

Nielsen and Callaghan (2003) have recently applied Eq. (2) for rough turbulent flow to include the effect of streaming in shear stress and sediment transport calculations for sheet flow under waves. Following this approach smooth turbulent flow will be considered using Myrhaug's (1995) smooth bed friction factor given by

$$f_{\mathrm{w}} = rRe^{-s} \quad \text{for } Re \gtrsim 3 \times 10^5 \tag{5}$$

with the coefficients

$$(r, s) = (0.0450, 0.175) \tag{6}$$

Alternative friction factors for smooth turbulent flow proposed by Jonsson (1980), Fredsøe and Deigaard (1992), Soulsby (1997) and Samad (2000) are given by Eq. (5) with (r, s) values given in Table 3.

Thus the friction factors for laminar and smooth turbulent flow have the form $f_{\mathrm{w}} = rRe^{-s}$.

The method of applying the laminar flow result in Eq. (2), and to replace the friction factor by that for smooth turbulent flow, should be considered as a first approximation to the streaming related shear stress for smooth turbulent flow. This is encouraged by the success of Nielsen and Callaghan (2003) in predicting the total sediment transport rate data of Ribberink et al. (2000). However, this approach should be validated by, e.g. using a full boundary layer model.

2.2. Probability distribution of bottom shear stress maxima

The present approach is based on the following assumptions:

(1) the free surface elevation $\zeta(t)$ is a stationary Gaussian narrow-band random process with zero expectation described by the single-sided spectral density $S_{\zeta\zeta}(\omega)$,
(2) the bottom friction formula for regular waves given in Section 2.1, is valid for irregular waves as well.

The second assumption implies that each wave is treated individually, and consequently that the bottom friction is taken to be constant for a given wave situation. The accuracy of this assumption has been justified by Samad (2000) for laminar and smooth turbulent boundary layer flow, for which the bottom friction is given by $\tau_w/\rho = 0.5 f_w U^2$. Here f_w is given in Eq. (3) for laminar flow, and by Eq. (5) using $(r, s) = (0.041, 0.16)$ for smooth turbulent flow. Samad (2000) found good agreement between his measured bed shear stresses (laminar and smooth turbulent) under irregular waves and simulations of bed shear stresses based on individual wave formulas. The bottom friction formula related to streaming is essentially based on the laminar and smooth turbulent bed friction factors. Thus, for linear waves the assumption of treating each wave individually is justified. The accuracy of the narrow-band assumption will be discussed below.

Based on the present assumptions, the time-dependent near-bed orbital displacement $a(t)$ and velocity $u(t)$, are both stationary Gaussian narrow-band processes with zero expectations and with single-sided spectral densities as follows:

$$S_{aa}(\omega) = \frac{S_{\zeta\zeta}(\omega)}{\sinh^2 kh} \tag{7}$$

$$S_{uu}(\omega) = \omega^2 S_{aa}(\omega) = \frac{\omega^2 S_{\zeta\zeta}(\omega)}{\sinh^2 kh} \tag{8}$$

For a narrow-band process the waves are specified as a ‘harmonic’ wave with cyclic frequency ω and with slowly varying amplitude and phase. Then, for the first order, the near-bed orbital velocity amplitude U is related to the near-bed orbital displacement amplitude A by $U = \omega A$, where U is slowly varying with t as well (see e.g. Sveshnikov, 1966).

It follows from the narrow-band assumption that the near-bed orbital displacement amplitude, A, and the near-bed orbital velocity amplitude, U, are Rayleigh-distributed with the cumulative distribution function given as follows

$$P(\hat{x}) = 1 - \exp(-\hat{x}^2); \quad \hat{x} = x/x_{\mathrm{rms}} \geq 0 \tag{9}$$

where x represents A or U, and x_{rms} is the rms value of x representing A_{rms} or U_{rms}.

When $\hat{x}$ is Rayleigh-distributed, and $\hat{x}$ is defined within a finite interval $\hat{x}_1 \leq \hat{x} \leq \hat{x}_2$, then $\hat{x}$ follows the truncated Rayleigh distribution with the cumulative distribution function given as follows:

$$P(\hat{x}) = \frac{\exp(-\hat{x}_1^2) - \exp(-\hat{x}^2)}{\exp(-\hat{x}_1^2) - \exp(-\hat{x}_2^2)}; \quad \hat{x}_1 \le \hat{x} \le \hat{x}_2 \tag{10}$$

Now A_{rms} and U_{rms} are related to the zeroth moments m_{0aa} and m_{0uu} of the amplitude and velocity, respectively (corresponding to the variances of the amplitude (σ_{aa}^2) and the velocity (σ_{uu}^2)), given as follows:

$$A_{\mathrm{rms}}^2 = 2m_{0aa} = 2\sigma_{aa}^2 = 2\int_0^\infty S_{aa}(\omega)\mathrm{d}\omega \tag{11}$$

$$U_{\mathrm{rms}}^2 = 2m_{0uu} = 2\sigma_{uu}^2 = 2\int_0^\infty S_{uu}(\omega)\mathrm{d}\omega \tag{12}$$

It should be noted that U_{rms} used by Soulsby (1997) corresponds to the standard deviation σ_{uu} used here.

From Eqs. (12) and (8), it also appears that $m_{0uu} = m_{2aa}$, where $m_{2aa} = \int_0^\infty \omega^2 S_{aa}(\omega)\mathrm{d}\omega$ is the second moment of the amplitude spectral density. Thus, the mean zero-crossing frequency for the near-bed orbital displacement, ω_z, is obtained from the spectral moments of $a(t)$ as follows

$$\omega_z = \left(\frac{m_{2aa}}{m_{0aa}}\right)^{1/2} = \left(\frac{m_{0uu}}{m_{0aa}}\right)^{1/2} = \frac{U_{\mathrm{rms}}}{A_{\mathrm{rms}}} \tag{13}$$

where Eqs. (11) and (12) have been used. This result is valid for a stationary Gaussian random process. Note that for a finite-band process this zero-crossing frequency of $a(t)$ at the bed generally will be smaller than the zero-crossing frequency of $\zeta(t)$ at the surface due to greater attenuation of high frequencies; this means that the high wave frequency components will not reach the bottom. However, for a narrow-band process these zero-crossing frequencies will be equal, since there is only one frequency present.

For a narrow-band process, $A = U/\omega$ where ω is replaced by ω_z from Eq. (13) and A is given as follows: $A = UA_{\mathrm{rms}}/U_{\mathrm{rms}}$. Then, by substituting this in Eq. (2) using Eqs. (5) and (4), Eq. (2) can be re-arranged to give the streaming-related bottom shear stress for the individual narrow-band random wave-cycles as follows

$$\frac{\tau_{\mathrm{str}}}{\rho} = \frac{\bar{\tau}_{\mathrm{str\ rms}}}{\rho}\left(\frac{U}{U_{\mathrm{rms}}}\right)^{3-2s} \tag{14}$$

where, by definition,

$$\frac{\bar{\tau}_{\mathrm{str\ rms}}}{\rho} = \frac{1}{4\sqrt{2}}\bar{k}A_{\mathrm{rms}}U_{\mathrm{rms}}^2 r Re_{\mathrm{rms}}^{-s}; \quad Re_{\mathrm{rms}} = \frac{U_{\mathrm{rms}}A_{\mathrm{rms}}}{\nu} \tag{15}$$

and $\bar{k}$ is the wave number corresponding to ω_z determined from $\omega_z^2 = g\bar{k}\tanh \bar{k}h$. By introducing $\hat{\tau}_{\mathrm{str}} = \tau_{\mathrm{str}}/\bar{\tau}_{\mathrm{str\ rms}}$ and $\hat{U} = U/U_{\mathrm{rms}}$ in Eq. (14), Eq. (14) can be re-arranged to give the shear stress related to streaming for individual narrow-band random waves as follows:

$$\hat{\tau}_{\mathrm{str}} = \hat{U}^{3-2s} \tag{16}$$

Now the cumulative distribution function of $\hat{\tau}_{\mathrm{str}}$ follows by transformation of random variables when $\hat{U}(\hat{\tau}_{\mathrm{str}})$ is known. By utilizing that $p(\hat{\tau}_{str}) = p(\hat{U})|\mathrm{d}\hat{U}/\mathrm{d}\hat{\tau}|$ and by using Eq. (9) with $\hat{x} = \hat{U}$, the probability density functions of the non-dimensional shear stress for the two flow regimes are given as follows:

$$p(\hat{\tau}_{\mathrm{str}}) = \exp(-\hat{\tau}_{\mathrm{str}}); \quad \hat{\tau}_{\mathrm{str}} \geq 0, \ \text{laminar} \tag{17}$$

$$p(\hat{\tau}_{\mathrm{str}}) = \beta \hat{\tau}_{\mathrm{str}}^{\beta-1} \exp(-\hat{\tau}_{\mathrm{str}}^{\beta}); \quad \hat{\tau}_{\mathrm{str}} \geq 0, \ \beta = \frac{2}{3-2s}, \ \text{smooth} \tag{18}$$

The corresponding cumulative distribution functions for the two flow regimes are given as follows:

$$P(\hat{\tau}_{\mathrm{str}}) = 1 - \exp(-\hat{\tau}_{\mathrm{str}}); \quad \hat{\tau}_{\mathrm{str}} \geq 0, \ \text{laminar} \tag{19}$$

$$P(\hat{\tau}_{\mathrm{str}}) = 1 - \exp(-\hat{\tau}_{\mathrm{str}}^{\beta}); \quad \hat{\tau}_{\mathrm{str}} \geq 0, \ \beta = \frac{2}{3-2s}, \ \text{smooth} \tag{20}$$

Hence the distribution of $\hat{\tau}_{\mathrm{str}}$ is given by an exponential distribution for laminar flow and a Weibull distribution for smooth turbulent flow.

These results are based on the not truncated Rayleigh distribution in Eq. (9) (rather than using the truncated distribution in Eq. (10)), which are sound for practical applications (see Appendix A for details).

2.3. Some characteristic statistical values

When the cumulative distribution function is known, the relevant characteristic statistical values of the bed shear stress related to streaming for individual random waves can be calculated. Here only a few characteristic statistical values will be discussed, based on the cumulative distribution functions in Eqs. (19) and (20).

The rms value is given as follows:

$$\hat{\tau}_{\mathrm{str\ rms}} \equiv (E[\hat{\tau}_{\mathrm{str}}^2])^{1/2} = \sqrt{2}, \ \text{laminar} \tag{21}$$

$$\hat{\tau}_{\mathrm{str\ rms}} = \left[\Gamma\left(1 + \frac{2}{\beta}\right)\right]^{1/2} = [\Gamma(4-2s)]^{1/2}, \ \text{smooth} \tag{22}$$

The value of $\hat{\tau}_{\mathrm{str}}$ which is exceeded by the probability $1/n$ is given as follows:

$$\hat{\tau}_{\mathrm{str}\ 1/n} = \ln n, \ \text{laminar} \tag{23}$$

$$\hat{\tau}_{\mathrm{str}\ 1/n} = (\ln n)^{1/\beta} = (\ln n)^{(3-2s)/2}, \ \text{smooth} \tag{24}$$

The validity ranges for $\hat{\tau}_{\mathrm{str\ rms}}$ and $\hat{\tau}_{\mathrm{str}\ 1/n}$ with $n = 3$, 10 are summarized in Table 1 for laminar flow and in Table 2 for smooth turbulent flow.

Table 1
Validity ranges of the stochastic approach for bottom friction caused by boundary layer streaming, linear waves and second order Stokes waves for laminar flow, based on an overprediction of less than about 10% by the not truncated vs. the truncated distribution

Streaming	$\hat{\tau}_{\mathrm{str\ rms}}$ (Eq. (21))		$Re_{\mathrm{rms}} \lesssim 7\times10^4$
	$\hat{\tau}_{\mathrm{str}\ 1/n}$ (Eq. (23))	$n=3$	$Re_{\mathrm{rms}} \lesssim 10^5$
		$n=10$	$Re_{\mathrm{rms}} \lesssim 8\times10^4$
Linear waves ($\Delta_{\mathrm{rms}}=0$)	$\hat{\tau}_{\mathrm{rms}}$ (Eq. (B11))		$Re_{\mathrm{rms}} \lesssim 10^5$
and second order Stokes	$\hat{\tau}_{1/n}$ (Eq. (B12))	$n=3$	$Re_{\mathrm{rms}} \lesssim 10^5$
waves		$n=10$	$Re_{\mathrm{rms}} \lesssim 10^5$

The effect of truncation on the rms value for laminar and smooth turbulent flow is discussed in Appendix A.

2.4. Friction factor

The friction factors based on characteristic statistical values of the shear stress related to streaming for individual random waves can be defined. The rms friction factor is commonly used and is defined as follows:

$$f_{\mathrm{w\ str,\ rms}} = \frac{(\tau_{\mathrm{str}}/\rho)_{\mathrm{rms}}}{\frac{1}{2}U_{\mathrm{rms}}^2} \tag{25}$$

A conventional calculation method of the friction factor for random waves is to replace the wave related quantities by their rms values in an otherwise deterministic approach, i.e. by an equivalent sinusoidal wave. These conventional results are obtained by substituting Eq. (3), or Eqs. (5) and (6), in Eq. (2) and replacing U and A with their rms-values, and taking $\omega=\omega_z$ and $k=\bar{k}$. This gives: $(\tau_{\mathrm{str}}/\rho)_{\mathrm{rms}} = (1/4\sqrt{2})\bar{k}A_{\mathrm{rms}}U_{\mathrm{rms}}^2 rRe_{\mathrm{rms}}^{-s}$, corresponding to Eq. (15). According to the definition in Eq. (25), the deterministic friction factor is as follows:

$$f_{\mathrm{w\ str,\ det}} = \frac{1}{2\sqrt{2}}\bar{k}A_{\mathrm{rms}} rRe_{\mathrm{rms}}^{-s} \tag{26}$$

Similarly, the result according to the present stochastic approach is obtained by substituting $\hat{\tau}_{\mathrm{str\ rms}} = \tau_{\mathrm{str}}/\bar{\tau}_{\mathrm{str\ rms}}$ in Eq. (21) using Eq. (15) for laminar flow, and in Eq. (22) using Eq. (15) for smooth turbulent flow. According to the definition in Eq. (25), the stochastic friction

Table 2
Validity ranges of the stochastic approach for bottom friction caused by boundary layer streaming as well as linear waves for smooth turbulent flow, based on an underprediction of less than about 10% by the not truncated vs. the truncated distribution

Streaming	$\hat{\tau}_{\mathrm{str\ rms}}$ (Eq. (22))		$Re_{\mathrm{rms}} \gtrsim 3\times10^6$
	$\hat{\tau}_{\mathrm{str}\ 1/n}$ (Eq. (24))	$n=3$	$Re_{\mathrm{rms}} \gtrsim 3\times10^6$
		$n=10$	$Re_{\mathrm{rms}} \gtrsim 2\times10^6$
Linear waves	$\hat{\tau}_{\mathrm{rms}}$ (Eq. (C4))		$Re_{\mathrm{rms}} \gtrsim 3\times10^6$
	$\hat{\tau}_{1/n}$ (Eq. (C5))	$n=3$	$Re_{\mathrm{rms}} \gtrsim 2\times10^6$
		$n=10$	$Re_{\mathrm{rms}} \gtrsim 10^6$

These results are based on using $s=0.175$ (Myrhaug, 1995).

factors in the two flow regimes are as follows:

$$f_{\text{w str, stoch}} = \bar{k}A_{\text{rms}}Re_{\text{rms}}^{-0.5}, \quad \text{laminar} \tag{27}$$

$$f_{w\text{ str, stoch}} = \frac{1}{2\sqrt{2}}\bar{k}A_{\text{rms}}rRe_{\text{rms}}^{-s}[(3-2s)\Gamma(3-2s)]^{1/2}, \quad \text{smooth} \tag{28}$$

Fig. 1 gives an example of results for laminar flow showing the stochastic and deterministic friction factors divided by $\bar{k}A_{\text{rms}}$ versus Re_{rms}. The two lower straight lines represent the stochastic results according to Eq. (27) as well as the deterministic results according to Eq. (26) with $(r, s) = (2, 0.5)$. It should be noted that the results for the stochastic approach according to Eq. (27) is valid for $Re_{\text{rms}} \lesssim 7\times10^4$, which is consistent with the results for the rms-value given in Table 1. Frictions factors based on other characteristic statistical values, e.g. $\hat{\tau}_{\text{str }1/n}$, will have similar behaviour as shown in Fig. 1. The validity ranges for the characteristic statistical values considered here are given in Table 1.

By combining Eq. (26) with $(r, s) = (2, 0.5)$ and Eq. (27), it appears that the stochastic to deterministic method ratio for the rms friction factor is given by the factor $\sqrt{2}$, showing that the stochastic approach gives about 40 percent larger shear stress related to streaming than obtained using the deterministic approach. This suggests that a stochastic approach is required for laminar flow.

Fig. 2 gives an example of results for smooth turbulent flow showing the stochastic and deterministic friction factors divided by $\bar{k}A_{\text{rms}}$ versus Re_{rms}. The two lower straight lines represent the stochastic results according to Eq. (28) as well as the deterministic results according to Eq. (26) with $(r, s) = (0.0450, 0.175)$. It should be noted that the results for the stochastic approach according to Eq. (28) is valid for $Re_{\text{rms}} \gtrsim 3\times10^6$, which is consistent with the results for the rms-value given in Table 2. Friction factors based on other

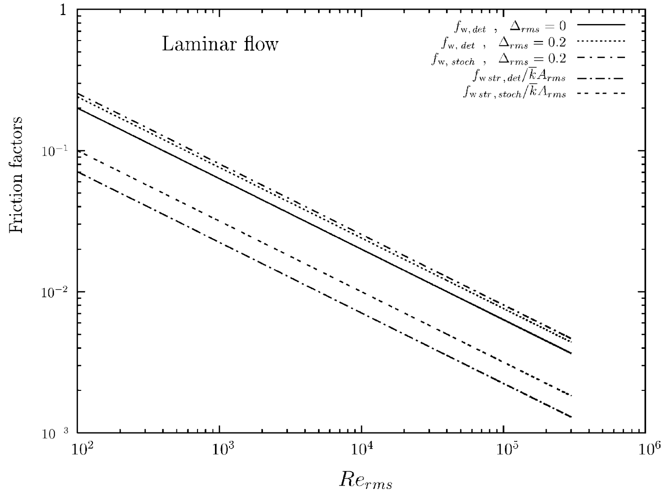

Fig. 1. Friction factors vs. Re_{rms} for laminar flow for given values of Δ_{rms}. Note that $f_{\text{w, det}}$ coincides with $f_{\text{w, stoch}}$ for $\Delta_{\text{rms}} = 0$. Note that the validity ranges are given from Table 1 as: $f_{\text{w str, det}}$, $f_{\text{w, det}}$, $Re_{\text{rms}} \lesssim 3\times10^5$; $f_{\text{w str, stoch}}$, $Re_{\text{rms}} \lesssim 7\times10^4$; $f_{\text{w, stoch}}$, $Re_{\text{rms}} \lesssim 10^5$.

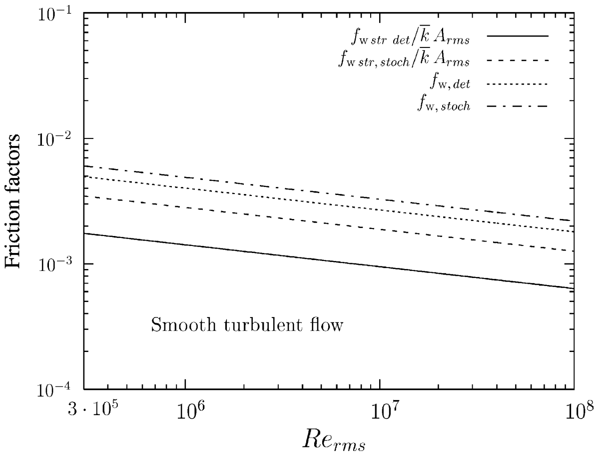

Fig. 2. Friction factors vs. Re_{rms} for smooth turbulent flow. Note that the validity ranges are given from Table 2 as: $f_{\mathrm{w\ str,\ det}}$, $f_{\mathrm{w,det}}$, $Re_{\mathrm{rms}} \gtrsim 3\times10^5$; $f_{\mathrm{w\ str,\ stoch}}$, $f_{\mathrm{w,stoch}}$, $Re_{\mathrm{rms}} \gtrsim 3\times10^6$.

characteristic statistical values, e.g. $\hat{\tau}_{\mathrm{str}\ 1/n}$, will have similar behaviour as shown in Fig. 2. The validity ranges for the characteristic statistical values considered here are given in Table 2.

By combining Eqs. (26) and (28), it appears that the stochastic to deterministic method ratio for the *rms* friction factor is given by

$$R_1 = [(3-2s)\Gamma(3-2s)]^{1/2} \tag{29}$$

By using the Myrhaug (1995) coefficients $(r, s)=(0.0450, 0.175)$, $R_1=1.98$, showing that the stochastic approach gives about two times larger shear stress related to streaming than obtained using the deterministic approach. This is also the case for the other models considered, see Table 3. This suggests that a stochastic approach is required for smooth turbulent flow.

The stochastic results for $\hat{\tau}_{\mathrm{str\ rms}}$ and $\hat{\tau}_{\mathrm{str}\ 1/n}$ according to Eqs. (22) and (24) using the coefficients (r, s) referred to in Section 2.1, are given in Table 4. It appears that all the models referred to in Table 3 give almost the same results. One should note that the results using Samad's (2000) coefficients coincide with those based on Fredsøe and Deigaard

Table 3
Stochastic to deterministic method ratios for the rms friction factor for streaming, R_1, and for linear waves, R_2, for smooth turbulent flow

Authors	Coefficients in friction factor		Streaming R_1 Eq. (29)	Linear waves R_2 Eq. (35)
	r	s		
Jonsson (1980)	0.09	0.2	1.93	1.20
Fredsøe and Deigaard (1992)	0.035	0.16	2.02	1.23
Samad (2000)	0.041	0.16	2.02	1.23
Myrhaug (1995)	0.0450	0.175	1.98	1.22
Soulsby (1997)	0.0521	0.187	1.96	1.21

Table 4
Bottom friction caused by boundary layer streaming and linear waves using four friction factors for smooth turbulent flow

Authors	Coefficients in friction factor		Streaming			Linear waves		
			$\hat{\tau}_{\text{str rms}}$ (Eq. (22))	$\hat{\tau}_{\text{str }1/n}$ (Eq. (24))		$\hat{\tau}_{\text{rms}}$ (Eq. (C4))	$\hat{\tau}_{1/n}$ (Eq. (C5))	
	r	s		$n=3$	$n=10$		$n=3$	$n=10$
Jonsson (1980)	0.09	0.2	1.93	1.130	2.96	1.20	1.078	1.95
Fredsøe and Deigaard (1992)	0.035	0.16	2.02	1.134	3.06	1.23	1.082	2.01
Samad (2000)	0.041	0.16	2.02	1.134	3.06	1.23	1.082	2.01
Myrhaug (1995)	0.0450	0.175	1.98	1.133	3.02	1.22	1.081	1.99
Soulsby (1997)	0.0521	0.187	1.96	1.131	2.99	1.21	1.079	1.97

(1992). It should also be noted that R_1 (Table 3) coincides with $\hat{\tau}_{\text{str rms}}$ (Table 4) with the present scaling.

3. Effects of streaming and second order Stokes waves versus effect of linear waves

Here the effect of streaming versus the effect of linear waves will be discussed. For laminar flow the effect of second order Stokes waves is also included. As for streaming, the results for linear waves and second order Stokes waves are based on the cumulative distribution functions which are not truncated. However, the truncated distribution functions determine the validity range of the not truncated results, which is the basis for the present practical method. Thus Appendix C gives a brief summary of the Myrhaug (1995) results for seabed shear stresses under linear random waves for smooth turbulent flow, plus an extension including the effect of truncation; Appendix B gives a brief summary of the Myrhaug and Holmedal (2003) results for seabed shear stresses under nonlinear second order random waves for laminar flow, plus an extension including the effect of truncation. Examples are included to illustrate the present method, and results are obtained using field data conditions.

3.1. Laminar bottom friction beneath nonlinear random waves

The rms friction factor obtained from the stochastic approach as well as the deterministic friction factor according to Myrhaug and Holmedal (2003) are given in Eqs. (B14) and (B16), respectively, in Appendix B as (see Appendix B for details)

$$f_{\text{w, stoch}} = 2Re_{\text{rms}}^{-0.5}(1 + 1.36\Delta_{\text{rms}}); \quad Re_{\text{rms}} \lesssim 10^5 \tag{30}$$

$$f_{\text{w, det}} = 2\,Re_{\text{rms}}^{-0.5}(1 + \Delta_{\text{rms}}); \quad Re_{\text{rms}} \lesssim 3 \times 10^5 \tag{31}$$

The stochastic and deterministic wave friction factors for laminar flow are shown in Fig. 1 versus Re_{rms} for linear ($\Delta_{\text{rms}}=0$) and nonlinear ($\Delta_{\text{rms}}=0.20$) waves. The two upper straight lines represent the stochastic results according to Eq. (30), as well as the deterministic friction factor according to Eq. (31). Note that the stochastic rms friction factor coincides with the deterministic friction factor for $\Delta_{rms}=0$. Friction factors based on other characteristic statistical values, e.g. $\hat{\tau}_{1/n}$, will have a similar behaviour as shown in Fig. 1. The validity ranges for the characteristic statistical values considered here are given in Table 1.

By combining Eqs. (30) and (31), it appears that the stochastic to deterministic method ratio R for the rms friction factor is given as

$$R=\frac{1+1.36\Delta_{rms}}{1+\Delta_{rms}} \tag{32}$$

This reveals that the deterministic approach gives the same result as the stochastic approach for linear waves ($\Delta_{rms}=0$); for second order Stokes waves $R=1.06$ when $\Delta_{rms}=0.20$. This suggests that for practical purposes the deterministic approach is applicable for laminar flow.

3.2. Smooth turbulent bottom friction beneath linear random waves

The rms friction factor obtained from the stochastic approach as well as the deterministic friction factor according to Myrhaug (1995) are given in Eqs. (C7) and (C8), respectively, in Appendix C as (see Appendix C for details)

$$f_{w,\ stoch}=rRe_{rms}^{-s}[\Gamma(3-2s)]^{1/2};\quad Re_{rms}\gtrsim 3\times 10^{6} \tag{33}$$

$$f_{w,\ det}=rRe_{rms}^{-s};\quad Re_{rms}\gtrsim 3\times 10^{5} \tag{34}$$

The stochastic and deterministic wave friction factors for smooth turbulent flow are shown in Fig. 2 versus Re_{rms}. The two upper lines represent the stochastic results according to Eq. (33), as well as the deterministic friction factor according to Eq. (34). Friction factors based on other characteristic statistical values, e.g. $\hat{\tau}_{1/n}$, will have a similar behaviour as shown in Fig. 2. The validity ranges for the characteristic statistical values considered here are given in Table 2.

By combining Eqs. (33) and (34), it appears that the stochastic to deterministic method ratio R_2 for the rms friction factor is given by

$$R_2=[\Gamma(3-2s)]^{1/2} \tag{35}$$

By using the Myrhaug (1995) coefficients $(r, s)=(0.0450, 0.175)$, $R_2=1.2$. This is also the case for the other models considered; see Table 3. This might suggest to use a stochastic approach for the cases where this accuracy is considered to be necessary. The results for $\hat{\tau}_{rms}$ and $\hat{\tau}_{1/n}$ according to Eqs. (C4) and (C5) using the coefficients (r, s) referred to in Section 2.1 are given in Table 4. It appears that the stochastic models give almost the same results. One should note that the results using Samad's (2000) coefficients coincide with those of Fredsøe and Deigaard (1992). It should also be noted that R_2 (Table 3) coincides with $\hat{\tau}_{rms}$ (Table 4) with the present scaling.

3.3. Streaming versus linear waves

Here the relative magnitude between the shear stress related to streaming and the shear stress under linear waves will be investigated for laminar and smooth turbulent flow. The shear stress for linear waves in shallow water for $\bar{k}h=\pi/10$ will be used as a reference value.

The rms value of the shear stress under linear waves is given as

$$\frac{\tau_{\mathrm{wrms}}}{\rho}=\frac{1}{2}r(\nu\omega_z)^s\left(\frac{\omega_z H_{\mathrm{rms}}}{2\sinh\bar{k}h}\right)^{2-2s}[\Gamma(3-2s)]^{1/2} \tag{36}$$

This result is obtained by combining Eqs. (C6) and (C7) (see Appendix C) and substitution of $A_{\mathrm{rms}}=U_{\mathrm{rms}}/\omega_z$ and

$$U_{\mathrm{rms}}=\frac{\omega_z H_{\mathrm{rms}}}{2\sinh\bar{k}h} \tag{37}$$

In shallow water, for which $\sinh\bar{k}h\approx\bar{k}h$ and taking $\bar{k}h=\pi/10$, Eq. (36) takes the form

$$\frac{\tau_{\mathrm{wrms}}}{\rho}=\frac{1}{2}r(\nu\omega_z)^s\left(\frac{\omega_z H_{\mathrm{rms}}}{2\pi/10}\right)^{2-2s}[\Gamma(3-2s)]^{1/2} \tag{38}$$

By combining Eqs. (25) and (28), and substitution of U_{rms} from Eq. (37), the rms value of the shear stress caused by streaming is given as

$$\frac{\tau_{\mathrm{str\ rms}}}{\rho}=[(3-2s)\Gamma(3-2s)]^{1/2}\frac{1}{4\sqrt{2}}\bar{k}A_{\mathrm{rms}}r(\nu\omega_z)^s\left(\frac{\omega_z H_{\mathrm{rms}}}{2\sinh\bar{k}h}\right)^{2-2s} \tag{39}$$

A measure of the relative magnitude between the effects of streaming in an arbitrary water depth and linear waves in shallow water R_{3*} is obtained by taking the ratio of Eqs. (39) and (38), which for laminar ($s=0.5$) and smooth turbulent flow give

$$R_{3*}=\frac{1}{2}\bar{k}A_{\mathrm{rms}}\frac{\pi/10}{\sinh\bar{k}h},\quad \text{laminar} \tag{40}$$

$$R_{3*}=\frac{(3-2s)^{1/2}}{2\sqrt{2}}\bar{k}A_{\mathrm{rms}}\left(\frac{\pi/10}{\sinh\bar{k}h}\right)^{2-2s},\quad \text{smooth} \tag{41}$$

Moreover, the ratio between the shear stress under linear waves in arbitrary water depth and in shallow water R_4 is obtained by taking the ratio of Eqs. (36) and (38), which gives

$$R_4=\frac{\pi/10}{\sinh\bar{k}h},\quad \text{laminar} \tag{42}$$

$$R_4=\left(\frac{\pi/10}{\sinh\bar{k}h}\right)^{2-2s},\quad \text{smooth} \tag{43}$$

The range of values of $\bar{k}A_{\mathrm{rms}}$ is determined by the validity of linear wave theory, which can be expressed in terms of the Ursell number as $H(2\pi/k)^2/h^3\lesssim 15$ for regular waves (Skovgaard et al., 1974). This criterion can be re-arranged to $(kH/2)/(kh)^3\lesssim 0.2$, which for narrow-band random waves is taken as $(\bar{k}H_{rms}/2)/(\bar{k}h)^3 \lesssim 0.2$, where $\bar{k}H_{rms}/2 = \bar{k}A_{rms} \sinh \bar{k}h$. Thus the Ursell number criterion can be re-arranged to

$$\bar{k}A_{rms} \lesssim 0.2 \frac{(\bar{k}h)^3}{\sinh \bar{k}h} \tag{44}$$

Moreover, the maximum steepness of regular waves in finite water depth is limited by the Miche breaking criterion, i.e. $kH/2 \leq \pi \times 0.142 \tanh(0.875kh)$ (see e.g. Soulsby, 1997). For narrow-band random waves this criterion can be re-arranged to

$$\bar{k}A_{rms} \leq \pi \times 0.142 \frac{\tanh(0.875\bar{k}h)}{\sinh \bar{k}h} \tag{45}$$

In the shallow water ($\bar{k}h = \pi/10$) to deep water ($\bar{k}h = \pi$) range it appears that Eq. (44) is the most restrictive for $\pi/10 \leq \bar{k}h \lesssim 1.2$, while Eq. (45) is the most restrictive for $1.2 \lesssim \bar{k}h \leq \pi$. Here the shallow to intermediate water depth range $\pi/10 \leq \bar{k}h \lesssim 1.2$ is considered, because the seabed shear stress is of most interest in this range. Thus $\bar{k}A_{rms}$ is restricted by Eq. (44) which for $\bar{k}h = (\pi/10, 1.2)$ gives $\bar{k}A_{rms} \lesssim (0.02, 0.23)$. However, since random waves are considered it can be argued that the criteria in Eqs. (44) and (45) should be based on the maximum wave within the time series, i.e. the maximum values of H and A within the time series should be used rather than the rms values. Since H and A are Rayleigh-distributed, $(H_{max}, A_{max}) = (H_{rms}, A_{rms})\sqrt{\ln N}$, where N is the number of waves within the time series. One should note that a time series of 1 h duration with a mean zero-crossing wave period of 10 s contains 360 individual waves, i.e. $N = 360$, which gives $A_{max} \approx 2.4A_{rms}$, and similarly for H_{max}. In this case the factors used in Eqs. (44) and (45) should be divided by the factor 2.4. Consequently, $\bar{k}A_{rms}$ will be restricted by the modified Eq. (44), which for $\bar{k}h = (\pi/10, 1.2)$ gives $\bar{k}A_{rms} \lesssim (0.01, 0.10)$. Although it is uncertain which values of H and A should be used in the criteria, the present discussion suggests that $\bar{k}A_{rms} = 0.20$ represents an upper limit.

The range of Δ_{rms} values follows by substituting the upper limit of $\bar{k}A_{rms}$ from Eq. (44) in Eq. (B5), which for $\bar{k}h = (\pi/10, 1.2)$ gives $\Delta_{rms} \lesssim (0.2, 0.1)$. However, if the criterion in Eq. (44) is based on the maximum wave in a time series of 1 h duration, then these values of Δ_{rms} should be divided by the factor of 2.4. Due to the uncertainty related to which values of A to use in the criterion in Eq. (44), it is suggested that $\Delta_{rms} = 0.2$ represents an upper limit.

An estimate of the upper limit of the relative magnitude between the effects of streaming for $\bar{k}h$ in the range $\pi/10$ to 1.2 and linear waves in shallow water R_3 can be obtained by substituting the upper limit of $\bar{k}A_{rms}$ from Eq. (44) in Eqs. (40) and (41), which gives

$$R_3 = \frac{\pi}{100} \frac{(\bar{k}h)^3}{\sinh^2 \bar{k}h}, \quad \text{laminar} \tag{46}$$

$$R_3 = \frac{(3-2s)^{1/2}}{2\sqrt{2}} 0.2 \frac{(\bar{k}h)^3}{\sinh \bar{k}h} \left(\frac{\pi/10}{\sinh \bar{k}h}\right)^{2-2s}, \quad \text{smooth} \tag{47}$$

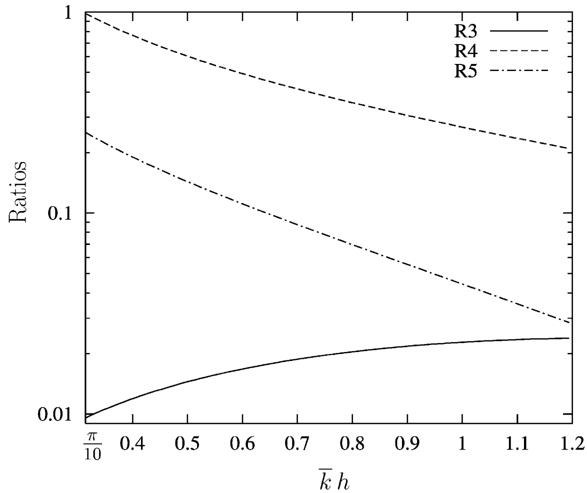

Fig. 3. The ratios R_3 (Eq. (46)), R_4 (Eq. (42)) and R_5 (Eq. (49)) versus $\bar{k}h$ for laminar flow.

Fig. 3 shows the ratios R_3 and R_4 versus $\bar{k}h$ in the range $\pi/10$ to 1.2 for laminar flow according to Eqs. (46) and (42), respectively. It appears that the ratio between the shear stress related to streaming (hereafter referred to as the streaming effect) and the shear stress under linear waves (hereafter referred to as the linear effect) in shallow water (R_3) increases from 0.01 to about 0.02 from shallow to the intermediate water depth considered here. One should note that the reason for this increase in R_3 as $\bar{k}h$ increases is caused by the validity range of linear wave theory given by the Ursell number criterion in Eq. (44). A consequence of this is that the maximum of R_3 becomes twice as large in intermediate than in shallow water. The ratio R_4 shows that the linear effect in intermediate water ($\bar{k}h = 1.2$) is only 20% of that in shallow water ($\bar{k}h = \pi/10$). By combining R_3 and R_4 it appears that the relative magnitude between the streaming effect and the linear effect increases from 1% in shallow water to 10% in intermediate water. For laminar flow the physical implication of this for, e.g. the dissipation of wave energy for progressive linear waves is that: in shallow water the streaming effect is 1% of the linear effect; in intermediate water the streaming effect increases by a factor of 2 relative to that in shallow water, and it is 10% of the linear effect in intermediate water; the sum of the linear and streaming effects in intermediate water is about 20% of the linear effect in shallow water.

Fig. 4 shows the ratios R_3 and R_4 versus $\bar{k}h$ in the range $\pi/10$ to 1.2 for smooth turbulent flow according to Eqs. (47) and (43), respectively, for the four friction factors considered. Overall, each model gives similar results. It appears that R_3 has a value close to 0.01; nearly invariant with $\bar{k}h$, which is caused by the validity range of linear wave theory given by the Ursell number criterion in Eq. (44). The ratio R_4 is reduced by a factor of about 10 from shallow to intermediate water depth. Thus the relative magnitude between the streaming effect and the linear effect increases from 0.01 in shallow water to about 0.1 in intermediate water. This is the same as for laminar flow. For smooth turbulent flow the physical implication of this for, e.g. the dissipation of wave energy for progressive linear waves is that: in shallow water the streaming effect is 1% of the linear effect;

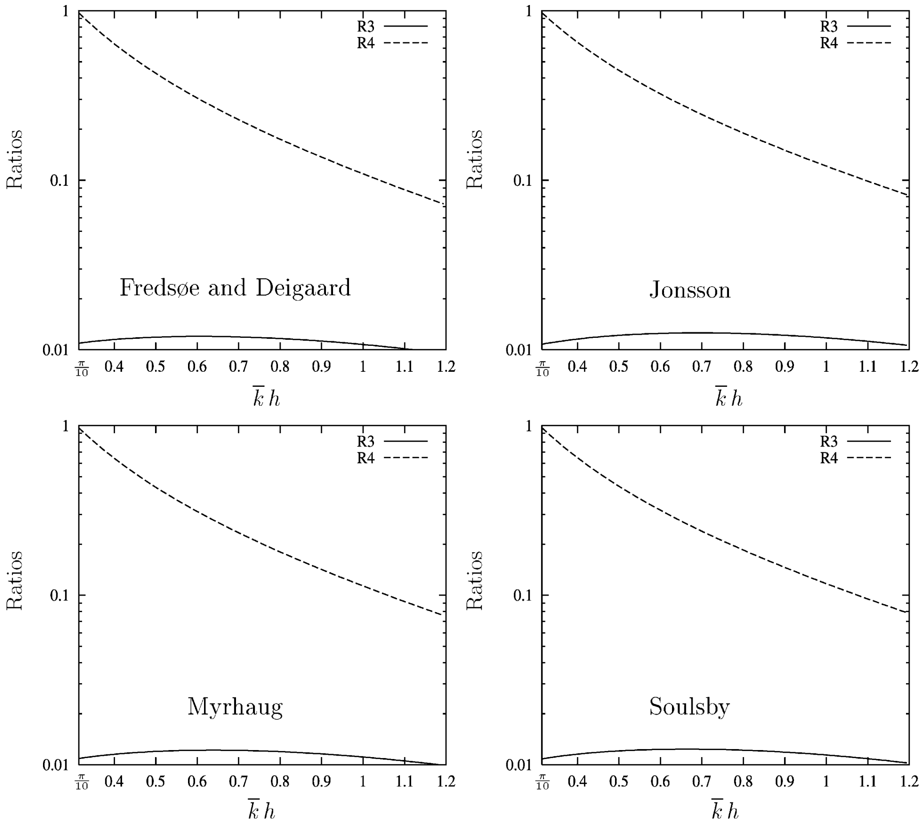

Fig. 4. The ratios R_3 (Eq. (47)) and R_4 (Eq. (43)) versus $\bar{k}h$ for smooth turbulent flow.

in intermediate water the streaming effect is the same as in shallow water, and it is 10% of the linear effect; the sum of the linear and streaming effects in intermediate water is about 10% of the linear effect in shallow water.

It should be noted that the results in Figs. 3 and 4 for the rms values are similar to those obtained using a deterministic approach. This means that by using a deterministic approach the curve representing R_3 will be reduced by the factors $\sqrt{2}$ and $(3-2s)^{1/2}\approx 1.6$ for laminar and smooth turbulent flow, respectively, while R_4 will be the same.

3.4. Second order Stokes waves versus linear waves for laminar flow

Here the magnitude of the shear stress related to the second order term of second order Stokes waves for laminar flow will be considered. The shear stress for linear waves in shallow water will be used as a reference.

The rms value of the second order component of the shear stress under second order Stokes waves is given as $1.36\Delta_{\mathrm{rms}}Re_{\mathrm{rms}}^{-0.5}U_{\mathrm{rms}}^{2}$. This result is obtained by combining Eqs. (B3), (B10) and (B11). By substitution of U_{rms} from Eq. (37) and Δ_{rms} from Eq. (B5), as well as dividing by Eq. (38) for $s=0.5$, the ratio between the second order contribution to the shear stress amplitude of second order Stokes waves (hereafter referred to as the second order effect) in an arbitrary water depth and the shear stress amplitude related to linear waves in shallow water for laminar flow is

$$R_{5*} = 1.36\left(1 + \frac{1}{\pi}\right)\frac{3\bar{k}A_{\mathrm{rms}}}{2\sinh^3 \bar{k}h}\frac{\pi}{10} \tag{48}$$

An estimate of the upper limit of this ratio for $\bar{k}h$ in the range $\pi/10$ to 1.2 is obtained by substituting the upper limit of $\bar{k}A_{\mathrm{rms}}$ from Eq. (44) in Eq. (48), which gives

$$R_5 = 0.0845\frac{(\bar{k}h)^3}{\sinh^4 \bar{k}h} \tag{49}$$

One should note that Eq. (49) is strictly not valid close to $\bar{k}h = \pi/10$ due to the restriction of no secondary bump in the free surface profile of second order Stokes waves (see e.g. Dean and Dalrymple, 1984). However, for the sake of simplicity this is not elaborated further. The use of Eq. (49) close to $\bar{k}h = \pi/10$ is sufficient for the order of magnitude considerations made here.

The ratio R_5 versus $\bar{k}h$ in the range $\pi/10$ to 1.2 for laminar flow according to Eq. (49) is shown in Fig. 3. It appears that the ratio between the second order effect and the linear effect in shallow water decreases from 0.25 to about 0.03 from shallow to intermediate water. By combining R_4 and R_5 it appears the relative magnitude between the second order effect and the linear effect is about 0.2 in both shallow and intermediate water. Moreover, it appears that the second order effect is an order of magnitude larger than the streaming effect in shallow water, while these two effects are of the same order of magnitude in intermediate water. One should note that the results for R_5 in Fig. 3 for the rms values are similar to those obtained using a deterministic approach, i.e. the curve representing R_5 will be reduced by a factor of 1.36.

For laminar flow the physical implication of this for, e.g. the dissipation of wave energy is that: in shallow water the second order effect is an order of magnitude larger than the streaming effect, and the former is 25% of the linear effect; in intermediate water the second order and streaming effects are of the same order of magnitude, and each are about 10% of the linear effect; the sum of the linear, streaming and second order effects in intermediate water is about 25% of the linear effect in shallow water.

3.5. Example 1. Laminar flow

This example is included in order to show the detailed calculation procedure for laminar flow.

Given flow conditions for a smooth bed:

Water depth, $h = 5$ m
Significant wave height, $H_s = 0.65$ m
Mean wave period, $T_z = 6$ s

Kinematic viscosity of water at temperature 10 °C and salinity 35‰ (Soulsby, 1997), $\nu = 1.36 \times 10^{-6}$ m^2/s

Calculated quantities:

rms wave height, $H_{\mathrm{rms}} = H_s/\sqrt{2} = 0.46$ m
Mean wave frequency, $\omega_z = 2\pi/T_z = 1.047$ s^{-1}
$\bar{k}$ from dispersion relationship corresponding to ω_z, $\bar{k} = 0.165$ m^{-1}
Intermediate water depth since, $\bar{k}h = 0.83$
rms bed orbital velocity amplitude from Eq. (37), $U_{\mathrm{rms}} = 0.26$ m/s
rms bed orbital displacement amplitude, $A_{\mathrm{rms}} = U_{\mathrm{rms}}/\omega_z = 0.25$ m
$\bar{k}A_{\mathrm{rms}}$, $\bar{k}A_{\mathrm{rms}} = 0.041$ (i.e. $\lesssim 0.12$ from Ursell number criterion in Eq. (44))
rms Reynolds number, $Re_{\mathrm{rms}} = U_{\mathrm{rms}}A_{\mathrm{rms}}/\nu = 4.8 \times 10^4$ (i.e. in the laminar flow regime since $Re_{\mathrm{rms}} \lesssim 10^5$)

Streaming:

$\bar{\tau}_{\mathrm{str\ rms}}/\rho$ from Eq. (15) with $(r, s) = (2, 0.5)$, $\bar{\tau}_{\mathrm{str\ rms}}/\rho = 4.47 \times 10^{-6}$ m^2/s^2
$f_{\mathrm{w\ str,\ det}}$ from Eq. (26) with $(r, s) = (2, 0.5)$, $f_{\mathrm{w\ str,\ det}} = 1.32 \times 10^{-4}$
$f_{\mathrm{w\ str,\ stoch}}$ from Eq. (27) (i.e. $Re_{\mathrm{rms}} \lesssim 7 \times 10^4$), $f_{\mathrm{w\ str,\ stoch}} = 1.87 \times 10^{-4}$
Stochastic to deterministic method ratio for rms friction factor, 1.42
Ratio between effect of streaming and effect of linear waves in shallow water from Eq. (46), $R_3 = 0.021$
Ratio between effect of linear waves in finite and shallow water from Eq. (42), $R_4 = 0.34$

Second order waves:

$\tau_{\mathrm{wrms}}/\rho$ from Eq. (B3), $\tau_{\mathrm{wrms}}/\rho = 3.1 \times 10^{-4}$ m^2/s^2
Δ_{rms} from Eq. (B5), $\Delta_{\mathrm{rms}} = 0.048$ (i.e. $\Delta_{\mathrm{rms}} < 0.20$)
$f_{\mathrm{w,\ det}}$ from Eq. (31), $f_{\mathrm{w,\ det}} = 9.57 \times 10^{-3}$
$f_{\mathrm{w,\ stoch}}$ from Eq. (30), $f_{\mathrm{w,\ stoch}} = 9.72 \times 10^{-3}$
$f_{\mathrm{w,\ det}}$ and $f_{\mathrm{w,\ stoch}}$ coincide for linear waves, given from Eq. (B15), $(f_{\mathrm{w,\ stoch}})_{\mathrm{lin}} = (f_{\mathrm{w,\ det}})_{\mathrm{lin}} = 9.13 \times 10^{-3}$
Stochastic to deterministic method ratio for rms friction factor from Eq. (32), $R = 1.02$
Nonlinear to linear ratios for characteristic values from Eq. (B13), $R_{2,\ \mathrm{rms}} = 1.07$, $R_{2,\ 1/3} = 1.05$, $R_{2,\ 1/10} = 1.07$
Ratio between effect of second order contribution and linear waves in shallow water from Eq. (49), $R_5 = 0.065$

3.6. Example 2. Smooth turbulent flow

This example is included in order to show the detailed calculation procedure for smooth turbulent flow. The results are based on the Myrhaug (1995) coefficients $(r, s) = (0.0450,$

0.175). It should be noted that smooth turbulent flow is of practical interest for flow over mud beds.

Given flow conditions for a smooth bed:

Water depth, $h = 15$ m
Significant wave height, $H_s = 7.5$ m
Mean wave period, $T_z = 8.9$ s
Kinematic viscosity of water at temperature 10 °C and salinity 35‰ (Soulsby, 1997), $\nu = 1.36 \times 10^{-6}$ m^2/s

Calculated quantities:

rms wave height, $H_{rms} = H_s/\sqrt{2} = 5.30$ m
Mean wave frequency, $\omega_z = 2\pi/T_z = 0.706$ s^{-1}
$\bar{k}$ from dispersion relationship corresponding to ω_z, $\bar{k} = 0.0667$ m^{-1}
Intermediate water depth, $\bar{k}h = 1.00$
rms bed orbital velocity amplitude from Eq. (37), $U_{rms} = 1.59$ m/s
rms bed orbital displacement amplitude, $A_{rms} = U_{rms}/\omega_z = 2.25$ m
$\bar{k}A_{rms}$, $\bar{k}A_{rms} = 0.15$ (i.e. $\lesssim 0.17$ from Ursell number criterion in Eq. (44))
rms Reynolds number, $Re_{rms} = U_{rms}A_{rms}/\nu = 2.63 \times 10^6$ (i.e. in the smooth turbulent flow regime since $Re_{rms} \gtrsim 3 \times 10^6$)

Streaming:

$\bar{\tau}_{str\ rms}/\rho$ from Eq. (15), $\bar{\tau}_{str\ rms}/\rho = 2.27 \times 10^{-4}$ m^2/s^2
$f_{w\ str,\ det}$ from Eq. (26), $f_{w\ str,\ det} = 1.80 \times 10^{-4}$
$f_{w\ str,\ stoch}$ from Eq. (28) (i.e. $Re_{rms} \gtrsim 3 \times 10^6$), $f_{w\ str,\ stoch} = 3.55 \times 10^{-4}$
Stochastic to deterministic ratio for rms friction factor from Eq. (29), $R_1 = 1.98$
Ratio between effect of streaming and effect of linear waves in shallow water from Eq. (47), $R_3 = 0.011$
Ratio between effect of linear waves in finite and shallow water from Eq. (43), $R_4 = 0.11$

Linear waves:

τ_{wrms}/ρ from Eq. (C3), $\tau_{wrms}/\rho = 4.28 \times 10^{-3}$ m^2/s^2
$f_{w,\ det}$ from Eq. (C8), $f_{w,\ det} = 3.39 \times 10^{-3}$
$f_{w,\ stoch}$ from Eq. (C7), $f_{w,\ stoch} = 4.13 \times 10^{-3}$
Stochastic to deterministic method ratio for rms friction factor from the ratio between Eqs. (C7) and (C8), 1.22.

4. Summary and conclusions

An approach is presented by which the effect of boundary layer streaming on the seabed shear stresses, beneath random waves, is investigated for laminar flow as well as smooth turbulent flow. It is demonstrated how bottom friction formulas for regular waves can be used to obtain the bed shear stresses resulting from steady streaming under random waves. As a result, friction factors for steady streaming under random waves are provided, and the effect of streaming versus the effect of linear waves is discussed. For laminar flow the effect of second order Stokes waves is also included. Comparisons are also made by using other friction factors for smooth turbulent flow. Finally, examples of the calculation procedure are given using data typical for field conditions. This is of practical interest for, e.g. flow over smooth and featureless beds as is frequently the case for freshly deposited muds, which are commonly taken to be smooth turbulent. The bed shear stresses enter in the calculation of, e.g. erosion and deposition of mud. The present analysis also has physical implications for, e.g. estimation of wave energy dissipation for flow above such beds.

The main conclusions are:

(a) For laminar and smooth turbulent flow the present stochastic approach gives about 40 percent and two times larger friction factors, respectively, than those obtained using rms values in an otherwise deterministic approach. This suggests that a stochastic approach is required for both laminar and smooth turbulent flow. For smooth turbulent flow this is valid for all the friction factors considered.

(b) The typical values exemplified for shallow ($\bar{k}h = \pi/10$) to intermediate ($\bar{k}h = 1.2$) water depths based on upper estimates of the rms values of the seabed shear stress, suggest that:

- For laminar and smooth turbulent flow the relative magnitude between the streaming effect and the linear effect increases from 1% in shallow water to 10% in intermediate water. This is because the streaming effect in intermediate water is about the same as in shallow water; this is a consequence of the upper validity range of linear wave theory given by the Ursell number criterion. Consequently, the sum of the linear and streaming effects in intermediate water is: 20% of the linear effect in shallow water for laminar flow, and 10% of the linear effect in shallow water for smooth turbulent flow. For smooth turbulent flow this is valid for all the friction factors considered.
- For laminar flow the second order effect is an order of magnitude larger than the streaming effect in shallow water, and the former is 25% of the linear effect. In intermediate water the second order effect and streaming effect are of the same order of magnitude; about 10% of the linear effect. The sum of the linear, streaming and second order effects in intermediate water is about 25% of the linear effect in shallow water.

Acknowledgements

This work was carried out as part of the SANDPIT project ‘Sand Transport and Morphology of Offshore Sand Mining Pits/Areas’, funded by the European Commission Research Directorate—General Contract No. EVK3-CT-2001-00056/SANDPIT.

Appendix A. Effect of truncation on bottom friction caused by boundary layer streaming

The cumulative distribution function of $\hat{\tau}_{str}$ follows by transformation of random variables when $\hat{U}(\hat{\tau}_{str})$ is known from Eq. (16). By utilizing that $p(\hat{\tau}_{str})=p(\hat{U})|d\hat{U}/d\hat{\tau}_{str}|$ and by using Eq. (10) with $\hat{x}=\hat{U}$, $\hat{x}_1=0$, $\hat{x}_2=\hat{U}_1$ for laminar flow, and $\hat{x}=\hat{U}$, $\hat{x}_1=\hat{U}_1$, $\hat{x}_2\to\infty$ for smooth turbulent flow, the probability density functions of the non-dimensional shear stress for the two flow regimes are given as follows

$$p(\hat{\tau}_{str}) = \frac{\exp(-\hat{\tau}_{str})}{1-\exp(-\hat{U}_1^2)}; \quad 0\le\hat{\tau}_{str}\le\hat{U}_1^2, \text{ laminar} \tag{A1}$$

$$p(\hat{\tau}_{str}) = \beta\hat{\tau}_{str}^{\beta-1}\exp(\hat{U}_1^2-\hat{\tau}_{str}^{\beta}); \quad \hat{\tau}_{str}\ge\hat{\tau}_1=\hat{U}_1^{2/\beta},\ \beta=\frac{2}{3-2s}, \text{ smooth} \tag{A2}$$

where $\hat{U}_1=(3\times10^5/Re_{rms})^{1/2}$, i.e. corresponding to the upper and lower limits of the laminar and smooth turbulent flow regimes, respectively. The cumulative distribution functions for the two flow regimes are given as follows:

$$P(\hat{\tau}_{str}) = \frac{1-\exp(-\hat{\tau}_{str})}{1-\exp(-\hat{U}_1^2)}; \quad 0\le\hat{\tau}_{str}\le\hat{U}_1^2, \text{ laminar} \tag{A3}$$

$$P(\hat{\tau}_{str}) = 1-\exp(\hat{U}_1^2-\hat{\tau}_{str}^{\beta}); \quad \hat{\tau}_{str}\ge\hat{\tau}_1, \text{ smooth} \tag{A4}$$

This shows that the distribution of $\hat{\tau}_{str}$ is given by a truncated exponential and a truncated Weibull distribution for laminar and smooth turbulent flow, respectively.

The rms value is given as follows:

$$\hat{\tau}_{str\ rms}\equiv(E[\hat{\tau}_{str}^2])^{1/2}=\sqrt{2}\left[\frac{1-\left(1+\hat{U}_1^2+\frac{1}{2}\hat{U}_1^4\right)e^{-\hat{U}_1^2}}{1-e^{-\hat{U}_1^2}}\right]^{1/2}, \text{ laminar} \tag{A5}$$

$$\hat{\tau}_{str\ rms}=\left[\Gamma\left(1+\frac{2}{\beta},\hat{U}_1^2\right)\right]^{1/2}e^{\hat{U}_1^2}, \text{ smooth} \tag{A6}$$

The value of $\hat{\tau}_{str}$ which is exceeded by the probability $1/n$ is given as follows:

$$\hat{\tau}_{str\ 1/n}=\ln n-\ln\left[1+(n-1)e^{-\hat{U}_1^2}\right], \text{ laminar} \tag{A7}$$

$$\hat{\tau}_{str\ 1/n}=(\ln n+\hat{U}_1^2)^{1/\beta}, \text{ smooth} \tag{A8}$$

The effect of truncation on the rms value for laminar flow is considered by the ratio between the quantities given in Eqs. (A5) and (21), and is denoted as $R_{str\ rms}$. The ratios for the $1/n$th values are denoted as $R_{str\ 1/n}$, and are given as the ratio between the quantities given in Eqs. (A7) and (23). Fig. A1 shows these ratios versus Re_{rms} in the range 10^4 to 3×10^5. It appears that the results for $\hat{\tau}_{str\ rms}$ which are not truncated, deviate less than about 10% from the truncated results for $Re_{rms}\lesssim7\times10^4$, which should be acceptable for

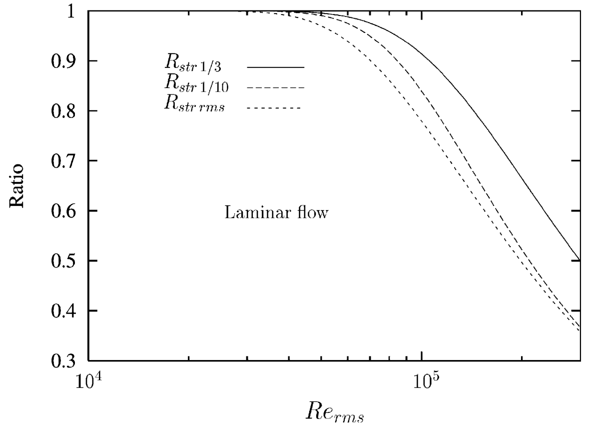

Fig. A1. The truncated to not truncated ratios for $\hat{\tau}_{\mathrm{str\ rms}}$ and $\hat{\tau}_{\mathrm{str}\ 1/n}$ with $n=3$, 10 vs. Re_{rms} for laminar flow.

practical purposes. Thus the range of validity, based on the distribution which is not truncated, is $Re_{\mathrm{rms}} \lesssim 7\times 10^4$. The validity ranges for $\hat{\tau}_{\mathrm{str\ rms}}$ and $\hat{\tau}_{\mathrm{str}\ 1/n}$ with $n=3$, 10 are summarized in Table 1.

The effect of truncation on the rms value for smooth turbulent flow is considered by the ratio between the quantities given in Eqs. (A6) and (22), and is denoted $R_{\mathrm{str\ rms}}$. The ratios for the $1/n$th values are denoted as $R_{\mathrm{str}\ 1/n}$, and are given as the ratio between the quantities given in Eqs. (A8) and (24). Fig. A2 shows these ratios versus Re_{rms} in the range 3×10^5 to 10^8 for $s=0.175$ (Myrhaug, 1995). It appears that the results for $\hat{\tau}_{\mathrm{str\ rms}}$ which are not truncated, deviate less than about 10% from the truncated results for $Re_{\mathrm{rms}} \gtrsim 3\times 10^6$, which should be acceptable for practical purposes. Thus the range of validity, based on the distribution which is not truncated, is $Re_{\mathrm{rms}} \gtrsim 3\times 10^6$. The validity ranges for $\hat{\tau}_{\mathrm{str\ rms}}$ and $\hat{\tau}_{\mathrm{str}\ 1/n}$ with $n=3$, 10 are summarized in Table 2.

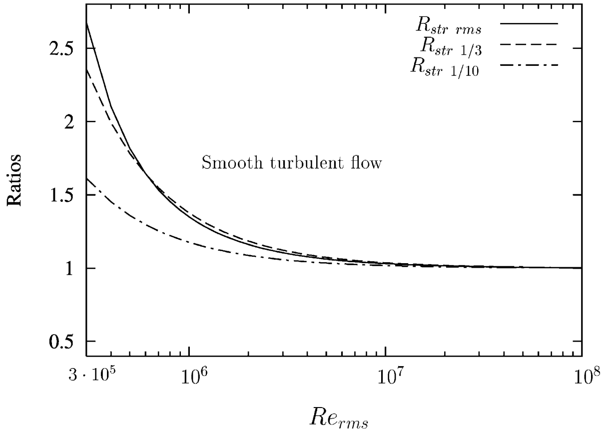

Fig. A2. The truncated to not truncated ratios for $\hat{\tau}_{\mathrm{str\ rms}}$ and $\hat{\tau}_{\mathrm{str}\ 1/n}$ with $n=3$, 10 vs. Re_{rms} for smooth turbulent flow.

Appendix B. Laminar bottom friction beneath nonlinear random waves including effect of truncation

Myrhaug and Holmedal (2003) based the approach essentially on the same assumptions as in Section 2.2, except for using the Damgaard et al. (1996) bottom friction formula for second order regular waves, which is assumed to be valid for second order nonlinear irregular waves as well. Similarly, the probability density function of the non-dimensional maximum bed shear stress, $\hat{\tau}$, was determined by transformation of random variables. One should note that the transformation was made by using the Rayleigh distribution in Eq. (9), rather than the truncated Rayleigh distribution in Eq. (10). Although the approach was an approximation, $\hat{\tau}_{\mathrm{rms}}$ and $\hat{\tau}_{1/n}$ for $n=3$, 10 are overpredicted by less than 10% for $Re_{\mathrm{rms}} \lesssim 10^5$ (i.e. covering the entire laminar flow regime), justifying the approach.

However, if the transformation is made correctly by using the truncated Rayleigh distribution in Eq. (10), then the probability density function of the non-dimensional maximum bed shear stress is given as follows

$$p(\hat{\tau}) = \frac{\frac{\sqrt{1+4\Delta_{\mathrm{rms}}\hat{\tau}}-1}{\Delta_{\mathrm{rms}}\sqrt{1+4\Delta_{\mathrm{rms}}\hat{\tau}}}\exp\left[-\frac{(\sqrt{1+4\Delta_{\mathrm{rms}}\hat{\tau}}-1)^2}{4\Delta_{\mathrm{rms}}^2}\right]}{1-\exp(-\hat{U}_1^2)}; \quad 0 \le \hat{\tau} \le \hat{\tau}_2 \tag{B1}$$

and with the cumulative distribution function

$$P(\hat{\tau}) = \frac{1-\exp\left[-\frac{(\sqrt{1+4\Delta_{\mathrm{rms}}\hat{\tau}}-1)^2}{4\Delta_{\mathrm{rms}}^2}\right]}{1-\exp(-\hat{U}_1^2)}; \quad 0 \le \hat{\tau} \le \hat{\tau}_2 \tag{B2}$$

where the maximum bottom shear stress, τ_{m}, is made dimensionless by τ_{wrms}, i.e.

$$\hat{\tau} = \frac{\tau_{\mathrm{m}}}{\tau_{\mathrm{wrms}}}; \quad \tau_{\mathrm{wrms}} = \rho Re_{\mathrm{rms}}^{-0.5} U_{\mathrm{rms}}^2 \tag{B3}$$

and

$$\hat{\tau}_2 = \hat{U}_1(1+\Delta_{\mathrm{rms}}\hat{U}_1); \quad \hat{U}_1 = \left(\frac{3\times 10^5}{Re_{\mathrm{rms}}}\right)^{1/2} \tag{B4}$$

By definition

$$\Delta_{\mathrm{rms}} = \left(1+\frac{1}{\pi}\right)\frac{3\bar{k}H_{\mathrm{rms}}}{8\sinh^3 \bar{k}h} = \left(1+\frac{1}{\pi}\right)\frac{3\bar{k}A_{\mathrm{rms}}}{4\sinh^2 \bar{k}h} \tag{B5}$$

and the rms wave height is given as

$$H_{\mathrm{rms}} = \left[8\int_0^{\infty} S_{\zeta\zeta}(\omega)\mathrm{d}\omega\right]^{1/2} \tag{B6}$$

One should note that Δ_{rms} represents a characteristic asymmetry of the shear stress in a sea state of random waves. Moreover, τ_{wrms} and Δ_{rms} are the quantities obtained by substituting the rms-values in the regular wave formulas. More details are given in Myrhaug and Holmedal (2003).

The rms-value is given as follows:

$$\hat{\tau}_{\mathrm{rms}} = \left[\int_0^{\hat{\tau}_2} \hat{\tau}^2 p(\hat{\tau}) \mathrm{d}\hat{\tau}\right]^{1/2} \tag{B7}$$

The value of $\hat{\tau}$ which is exceeded by the probability $1/n$ is given as follows:

$$\begin{aligned} \hat{\tau}_{1/n} = {} & \left\{\ln n - \ln\left[1 + (n-1)\mathrm{e}^{-\hat{U}_1^2}\right]\right\}^{1/2} \\ & \times\left(1 + \Delta_{\mathrm{rms}}\left\{\ln n - \ln\left[1 + (n-1)\mathrm{e}^{-\hat{U}_1^2}\right]\right\}^{1/2}\right); \quad Re_{\mathrm{rms}} \lesssim 3\times 10^5 \end{aligned} \tag{B8}$$

For linear waves ($\Delta_{\mathrm{rms}}=0$)

$$\hat{\tau}_{1/n} = \left\{\ln n - \ln\left[1 + (n-1)\mathrm{e}^{-\hat{U}_1^2}\right]\right\}^{1/2}; \quad Re_{\mathrm{rms}} \lesssim 3\times 10^5 \tag{B9}$$

The rms friction factor is defined as follows:

$$f_{\mathrm{w,\ rms}} = \frac{(\tau_{\mathrm{m}}/\rho)_{\mathrm{rms}}}{\frac{1}{2}U_{\mathrm{rms}}^2} \tag{B10}$$

By taking $\hat{U}_1$ (and $\hat{\tau}_2$) as infinitely large (i.e. by not truncating the distribution), Myrhaug and Holmedal (2003) obtained the following results

$$\hat{\tau}_{\mathrm{rms}} = 1 + 1.36\Delta_{\mathrm{rms}}; \quad Re_{\mathrm{rms}} \lesssim 10^5 \tag{B11}$$

and

$$\hat{\tau}_{1/n} = \sqrt{\ln n}(1 + \Delta_{\mathrm{rms}}\sqrt{\ln n}); \quad Re_{\mathrm{rms}} \lesssim 10^5 \tag{B12}$$

For linear waves Eqs. (B11) and (B12) reduce to $\hat{\tau}_{\mathrm{rms}}=1$ and $\hat{\tau}_{1/n}=\sqrt{\ln n}$, respectively.

B.1. Effect of truncation

The effect of truncation on the rms value is considered by the ratio between the quantities given in Eqs. (B7) and (B11), and is denoted as $R_{1,\ \mathrm{rms}}$. The ratios for the $1/n$th values are denoted as $R_{1,\ 1/n}$ and are given as the ratio between the quantities given in Eqs. (B8) and (B12). Fig. B1 shows these ratios versus Re_{rms} in the range 10^4 to 3×10^5 for $\Delta_{\mathrm{rms}}=0$, 0.05, 0.10, 0.15, 0.20. It appears that the results for $\hat{\tau}_{\mathrm{rms}}$, $\hat{\tau}_{1/3}$ and $\hat{\tau}_{1/10}$ which are not truncated, deviate less than about 10% from the truncated results for $Re_{\mathrm{rms}} \lesssim 10^5$, which should be acceptable for practical purposes. These results are consistent with the results in Myrhaug and Holmedal (2003), stating that Eqs. (B11) and (B12) are valid for $Re_{\mathrm{rms}} \lesssim 10^5$. The validity ranges for $\hat{\tau}_{\mathrm{rms}}$ and $\hat{\tau}_{1/n}$ with $n=3$, 10 are summarized in Table 1.

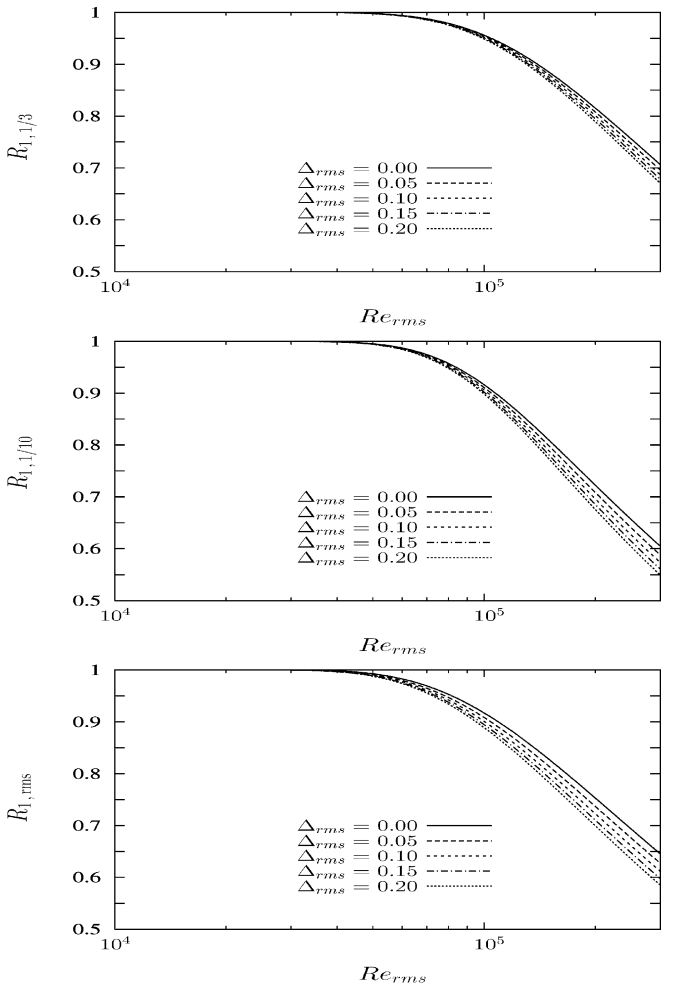

Fig. B1. The truncated to not truncated ratios for $\hat{\tau}_{\mathrm{rms}}$ and $\hat{\tau}_{1/n}$ with $n=3$, 10 vs. Re_{rms} for $\Delta_{\mathrm{rms}}=(0, 0.05, 0.10, 0.15, 0.20)$ for laminar flow.

B.2. Effect of nonlinearity

The effect of nonlinearity is investigated by comparing the results for nonlinear waves with those obtained for linear waves. For $\hat{\tau}_{\mathrm{rms}}$ and $\hat{\tau}_{1/n}$ these ratios are denoted as $R_{2,\ \mathrm{rms}}$ and $R_{2,\ 1/n}$, respectively. Fig. B2 shows the nonlinear to linear ratio results for $\hat{\tau}_{\mathrm{rms}}$ and $\hat{\tau}_{1/n}$ with $n=3$, 10 versus Δ_{rms} for $Re_{\mathrm{rms}}=10^4$, 5×10^4, 10^5, 3×10^5. For the range of Δ_{rms} values given here, it appears that the nonlinear to linear ratios for $\hat{\tau}_{\mathrm{rms}}$ and $\hat{\tau}_{1/n}$ vary from 1.0 to about 1.3 depending on Re_{rms} and n. This shows the importance of including nonlinear effects. The results for $Re_{\mathrm{rms}}=10^4$ can be taken as representative for the not

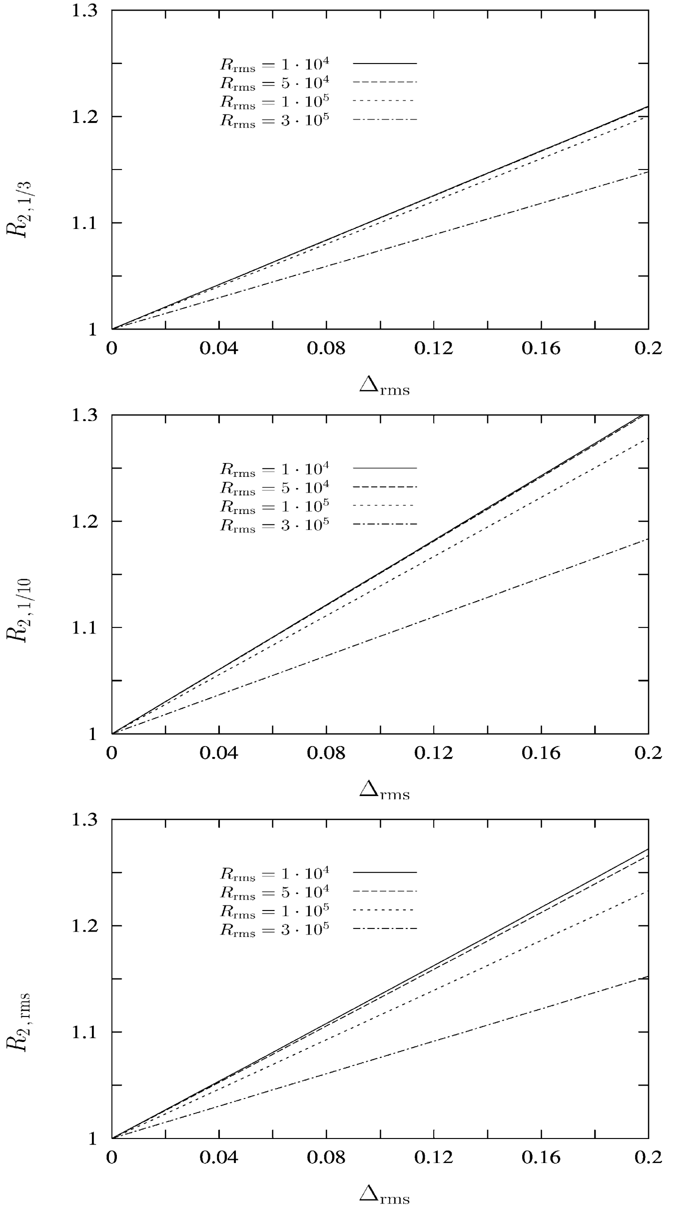

Fig. B2. Nonlinear to linear ratios of $\hat{\tau}_{\rm rms}$ and $\hat{\tau}_{1/n}$ with $n=3$, 10 vs. $\Delta_{\rm rms}$ for given values of $Re_{\rm rms}$ for laminar flow.

truncated distribution and are given by

$$(R_{2,\ \rm rms}, R_{2,1/3}, R_{2,1/10}) = 1 + (1.36, 1.05, 1.52)\Delta_{\rm rms} \tag{B13}$$

which were the results given in Myrhaug and Holmedal (2003).

B.3. Friction factor

Following Myrhaug and Holmedal (2003) the rms wave friction factor corresponding to the distribution which is not truncated, is given as

$$f_{\text{w, stoch}} = 2Re_{\text{rms}}^{-0.5}(1 + 1.36\Delta_{\text{rms}}); \quad Re_{\text{rms}} \lesssim 10^5 \tag{B14}$$

For linear waves ($\Delta_{\text{rms}} = 0$)

$$f_{\text{w, stoch}} = 2Re_{\text{rms}}^{-0.5} \tag{B15}$$

Similarly, the deterministic wave friction factor is given as

$$f_{\text{w, det}} = 2Re_{\text{rms}}^{-0.5}(1 + \Delta_{\text{rms}}); \quad Re_{\text{rms}} \lesssim 3\times 10^5 \tag{B16}$$

For linear waves the deterministic and stochastic results coincide, i.e. Eq. (B16) reduces to Eq. (B15).

Appendix C. Smooth turbulent bottom friction beneath linear random waves

Myrhaug (1995) based the approach on the same assumptions as in Section 2.2, and similarly the probability density function of the non-dimensional maximum bed shear stress, $\hat{\tau}$, was determined by transformation of random variables. One should note that the transformation was made by using the Rayleigh distribution in Eq. (9), rather than the truncated Rayleigh distribution in Eq. (10). Although the approach was an approximation, it will be shown here that $\hat{\tau}_{\text{rms}}$ is underpredicted by less than 10% for $Re_{\text{rms}} \gtrsim 3\times 10^6$ (i.e. covering the entire smooth turbulent flow regime), justifying the approach.

However, if the transformation is made correctly by using the truncated Rayleigh distribution in Eq. (10), then the probability density function of the non-dimensional maximum bed shear stress is given as follows

$$p(\hat{\tau}) = \beta\hat{\tau}^{\beta-1}\exp(\hat{U}_1^2 - \hat{\tau}^{\beta}); \quad \hat{\tau} \geq \hat{\tau}_1 = \hat{U}_1^{2/\beta}, \ \beta = \frac{1}{1-s} \tag{C1}$$

and with the cumulative distribution function

$$P(\hat{\tau}) = 1 - \exp(\hat{U}_1^2 - \hat{\tau}^{\beta}); \ \hat{\tau} \geq \hat{\tau}_1 \tag{C2}$$

where the maximum bottom shear stress, τ_{w}, is made dimensionless by τ_{wrms}, i.e.

$$\hat{\tau} = \frac{\tau_{\text{w}}}{\tau_{\text{wrms}}}; \ \tau_{\text{wrms}} = \frac{1}{2}\rho r Re_{\text{rms}}^{-s} U_{\text{rms}}^2 \tag{C3}$$

This shows that the distribution of $\hat{\tau}$ is given by a truncated Weibull distribution.

Now $\hat{\tau}_{\text{rms}}$ and $\hat{\tau}_{1/n}$ are given by Eqs. (A6) and (A8), respectively, in Appendix A with $\beta = 1/(1-s)$. By taking $\hat{U}_1$ (and $\hat{\tau}_1$) as zero (i.e. by not truncating the distribution), Myrhaug (1995) obtained the following results

$$\hat{\tau}_{\text{rms}} = [\Gamma(3-2s)]^{1/2} \tag{C4}$$

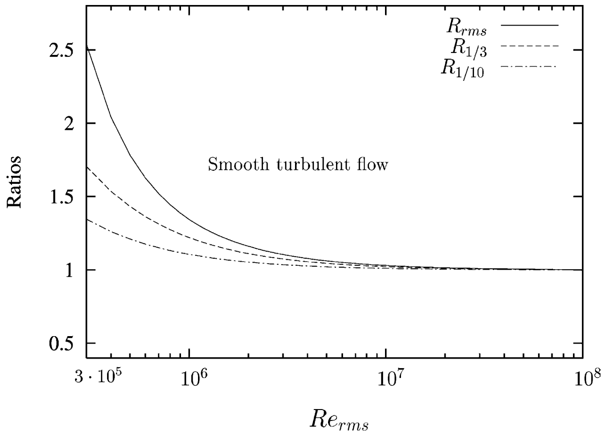

Fig. C1. The truncated to not truncated ratios for $\hat{\tau}_{\rm rms}$ and $\hat{\tau}_{1/n}$ with $n=3$, 10 vs. $Re_{\rm rms}$ for smooth turbulent flow.

and

$$\hat{\tau}_{1/n} = (\ln n)^{1-s} \tag{C5}$$

C.1. Effect of truncation

The effect of truncation on the *rms* value is considered by the ratio between the quantities given in Eq. (A6) with $\beta=1/(1-s)$ and Eq. (C4), and is denoted as $R_{\rm rms}$. The ratios for the $1/n$th values are denoted as $R_{1/n}$, and are given as the ratio between the quantities given in Eq. (A8) with $\beta=1/(1-s)$ and Eq. (C5). Fig. C1 shows these ratios versus $Re_{\rm rms}$ in the range 3×10^5 to 10^8. It appears that the results for $\hat{\tau}_{\rm rms}$ which are not truncated, deviate less than about 10% from the truncated results for $Re_{\rm rms}\gtrsim 3\times10^6$, which should be acceptable for practical purposes. Thus the range of validity, based on the distribution which is not truncated, is $Re_{\rm rms}\gtrsim 3\times10^6$. The validity ranges for $\hat{\tau}_{\rm rms}$ and $\hat{\tau}_{1/n}$ with $n=3$, 10 are summarized in Table 2.

C.2. Friction factor

The rms friction factor is defined as follows

$$f_{\rm w,\,rms} = \frac{(\tau_{\rm w}/\rho)_{\rm rms}}{\frac{1}{2}U_{\rm rms}^2} \tag{C6}$$

By substituting Eqs. (A6) and (C3) in Eq. (C6) the rms wave friction factor corresponding to the stochastic approach, can be obtained. The friction factor corresponding to the distribution which is not truncated is obtained as ($\hat{U}_1=0$, $\hat{\tau}_1=0$)

$$f_{\rm w,\,stoch} = rRe_{\rm rms}^{-s}\left[\Gamma\left(1+\frac{2}{\beta}\right)\right]^{1/2} = rRe_{\rm rms}^{-s}[\Gamma(3-2s)]^{1/2};\quad \beta=\frac{1}{1-s} \tag{C7}$$

Similarly, the deterministic wave friction factor is given as

$$f_{\mathrm{w,\,det}} = rRe_{\mathrm{rms}}^{-s}; \quad Re_{\mathrm{rms}} \gtrsim 3 \times 10^5 \tag{C8}$$

References

Damgaard, J.S., Stripling, S., Soulsby, R.L., 1996. Numerical modeling of coastal shingle transport. Report TR4, HR Wallingford, Wallingford, UK.

Davies, A.G., Villaret, C., 1997. Oscillatory flow over rippled beds: boundary layer structure and wave-induced Eulerian drift, In: Hunt, J.N. (Ed.), Gravity Waves in Water of Finite Depth. Advances in Fluid Mechanics, pp. 215–254 (Chapter 6).

Davies, A.G., Villaret, C., 1998. Wave-induced currents above rippled beds,In: Dronkers, J., Scheffers, M. (Eds.), Physics of Estuaries and Coastal Seas. A.A. Balkema, Rotterdam, pp. 187–199.

Davies, A.G., Villaret, C., 1999. Eulerian drift induced by progressive waves above rippled and very rough beds. J. Geophys. Res. 104 (C1), 1465–1488.

Dean, R.G., Dalrymple, R.A., 1984. Water Wave Mechanics for Engineers and Scientists. Prentice-Hall, New Jersey, USA.

Fredsøe, J., Deigaard, R., 1992. Mechanics of Coastal Sediment Transport. World Scientific, Singapore.

Jonsson, I.G., 1980. A new approach to oscillatory rough turbulent boundary layers. Ocean Eng. 7, 109–152 (err. 567–570).

Longuet-Higgins, M.S., 1956. The mechanics of the boundary layer near the bottom in a progressive wave, Proceedings of Sixth International Conference on Coastal Engineering. ASCE, Miami, pp. 184–193.

Myrhaug, D., 1995. Bottom friction beneath random waves. Coast. Eng. 24, 259–273.

Myrhaug, D., Holmedal, L.E., 2002. Bottom friction in nonlinear random waves plus current flow, Proceedings of the 28th International Conference on Coastal Engineering, vol. 1. ASCE, Cardiff, Wales, pp. 545–556.

Myrhaug, D., Holmedal, L.E., 2003. Laminar bottom friction beneath nonlinear random waves. Coast. Eng. J. 45 (1), 49–61.

Nielsen, P., 1992. Coastal Bottom Boundary Layers and Sediment Transport. World Scientific, Singapore.

Nielsen, P., Callaghan, D.P., 2003. Shear stress and sediment transport calculations for sheet flow under waves. Coast. Eng. 47 (3), 347–354.

Ribberink, J.S., Dohmen-Janssen, C.M., Hanes, D.M., McLean, S.R., Vincent, C., 2000. Near-bed sand transport mechanisms under waves, Proceedings of the 27th International Conference on Coastal Engineering. ASCE, Sydney, Australia, pp. 3263–3276.

Samad, M.A., 2000. Investigation of bottom boundary layer under irregular waves. PhD Thesis, Department of Civil Engineering, Tohoku University, Aoba, Sendai, Japan.

Schlichting, H., 1979. Boundary-Layer Theory, seventh ed. McGraw-Hill, New York.

Skovgaard, O., Svendsen, I.A., Jonsson, I.G., Brink-Kjær, O., 1974. Sinusoidal and cnoidal gravity waves formulae and tables. Institute of Hydrodynamics and Hydraulic Engineering (ISVA), Technical University of Denmark, Lyngby, Denmark.

Soulsby, R.L., 1997. Dynamics of Marine Sands. Thomas Telford, London, UK.

Sveshnikov, A.A., 1966. Applied Methods in the Theory of Random Functions. Pergamon Press, New York.

Whitehouse, R.J.S., Soulsby, R.L., Roberts, W., Mitchener, H., 2000. Dynamics of Estuaries Muds. Thomas Telford, London, UK.